PITCH GLIDE ANALYSIS AND SYNTHESIS FROM RECORDED TONES

Nelson Lee, Julius O. Smith III, Jonathan Abel and David Berners

CCRMA,
Stanford University
Stanford, USA
{nalee,jos,abel,dpberners}@ccrma.stanford.edu

ABSTRACT

Pitch glide is an important effect that occurs in nearly all plucked string instruments. In essence, large amplitude waves traveling on a string during the note onset increases the string tension above its nominal value, and therefore cause the pitch to temporarily increase. Measurements are presented showing an exponential relaxation of all the partial frequencies to their nominal values with a time-constant related to the decay rate of transverse waves propagating on the string. This exponential pitch trajectory is supported by a simple physical model in which the increased tension is somewhat counterbalanced by the increased length of the string. Finally, a method for synthesizing the plucked string via a novel hybrid digital waveguide-modal synthesis model is presented with implementation details for time-varying resonators.

1. INTRODUCTION

Tension modulation, the source of significant audible nonlinear effects in a vibrating string, has been thoroughly studied by acousticians, physicists as well as electrical engineers [1, 2, 3, 4, 5, 6, 7],

Pitch glide, commonly known in the literature as pitch variation, is the result of nonlinear interactions between the transverse vibration of a string and its tension. When a string is plucked at high amplitudes, the effective length of the string increases resulting in an increase in tension. It can be shown that the frequency of each mode of the system increases by approximately the same factor [8]. As observed from recorded data [9, 10, 11], the initial transient of a recorded tone exhibits audible pitch glide: the frequencies of the partials begin at greater values, and quickly approach their steady-state values.

Another significant musical effect resulting from tension modulation is nonlinear excitation/generation of missing modes as analyzed and shown experimentally in [5]. The excitation/generation of missing modes on a musical instrument such as the violin, is caused by a non-zero bridge admittance and angling of the string beyond the bridge, resulting in driving forces that occur at frequencies that are twice those of modes on the string. In our work, we address the first nonlinear effect: pitch glide.

In [9], pitch glide is estimated and modeled through tension modulation. Since actual tension modulation is oscillatory, they approximate it with a mean tension increase. As a result, a relationship between the mean tension and the effective fundamental frequency of the vibrating string over time, caused by changes in wave speed, is made. For synthesis, a digital waveguide model [12, 13, 14] with a time-varying fractional delay filter [15, 16, 17] is used to model the changing length of the string and thus the pitch glide exhibited at the onset of a plucked tone.

The main parameter estimated is the fractional delay value as a function of time, $d(n)$ in samples. As defined in Eq. 1, $d(n)$ is a function of $A = ES/F_{nom}$, where E is Young's Modulus, S is the cross sectional area of the string and F_{nom} is the nominal tension on the string at rest, L_{nom} is the nominal length of the string, $\hat{L}_{nom}$ is the rounded nominal string length and $L_{dev}(n)$, the change in length of the string with respect to the string at rest.

$$d(n) \approx -\frac{1}{2} \sum_{l=n-1-\hat{L}_{nom}}^{n-1} (1+A)\frac{L_{dev}(l)}{L_{nom}} \qquad (1)$$

Given a value for A, which can be computed from physical properties of the string, $L_{dev}(n)$ can be calculated. But as noted in [9] estimation of A and $L_{dev}(n)$ from recorded tones is non-trivial. During synthesis, elongation of the string may be computed through a sparse-squared-sum of delay-line values [9]. This work, on the other hand, makes use of the fact that pitch glide, for a plucked string, depends solely on the initial amplitude of the pluck. Furthermore, we implement the effects of a change in wave speed directly as modal resonators with time-varying frequencies, as opposed to modulation of the delay-line length. Due to limits of audio perception, it is only necessary to modulate the frequencies of the lower partials.

In [9], methods for estimation strive to only reproduce the effects of tension modulation and not to accurately estimate the physical properties of the string. Along similar lines, our work aims to reproduce pitch glide accurately for synthesis and not to obtain physical parameters of the string. Our synthesis model parametrizes pitch glide to accurately match our analyses of the observed pitch-variation per-partial of a recorded guitar tone. As the results show, our model is not only simple, but easy to estimate and is directly implemented in our synthesis model, an extension of the digital waveguide model similar to that proposed in [18]. Furthermore, our model and data of pitch glide fit that of the theory, as each partial exhibits the same pitch glide trajectory.

Other treatments of the effects of tension modulation have been made. In [19, 20], a conservation of energy formulation is given and different finite difference schemes with conditions for stability are investigated. In [21], investigation into aliasing resulting from varying delay line lengths using fractional delay filters is given. Since our synthesis model avoids changing delay line lengths in our digital waveguide, aliasing is not a concern for our model. [22] showed that energy conservation techniques can be extended to digital waveguide models using fractional allpass filters by reducing specific wave digital filters to simple first- and second-order all-pass filters.

In [23], a spatially distributed model of a nonlinear vibrating string is used in place of a digital waveguide to model tension

modulation on the string divided into segments. The delay line is replaced by first-order allpass sections to allow tension modulation to be modeled at any point along the string. The trade-off for the increase in modeling capability is efficiency, as what were previously shift operations are replaced with first-order filtering operations.

In [24], the functional transformation method is applied to a nonlinear vibrating string. Due to the nonlinearity, the method obtains only an implicit equation, not a multidimensional transfer function model as was obtained for the linear case, for implementation after inverse transformations and discretizations.

In Section 2, we present methods for analyzing a recorded tone and extracting pitch glide trajectories on a per-partial basis. In Section 3, we formulate an empirical model to match the pitch glide phenomenon observed from real data. In Section 3.1, we present methods for optimizing parameters of our model from recorded data. In Section 4, we discuss synthesis of pitch glide with a hybrid digital waveguide-modal synthesis model. and specific implementation issues and their resolution and we conclude with Section 5.

2. ANALYZING PITCH VARIATION

In this section, we briefly outline our methods for obtaining frequency trajectories on a per-partial basis and present the resulting data.

2.1. Bandpass Filtering for a Partial

For a recorded guitar tone, to observe partial i, we apply a bandpass filter to the original tone.

If H_{bp_i} is our bandpass filter for the ith partial and $x(t)$ is our recorded tone, we define the bandpassed signal as

$$x_i(t) = h_{bp,i} * x(t) \tag{2}$$

We chose to use a high-order FIR filter designed using the Parks-McClellan algorithm that had a 60dB magnitude drop outside of the pass-band, and a linear phase response within the pass-band. Since analysis occurs offline, we did not further investigate more efficient methods and filters for bandpass filtering for a single partial of a recorded tone. However, efficient structures for partial extraction have been investigated, as in [25], where a harmonic-extraction filter is introduced.

2.2. STFT and Quadratic Interpolation

Once $x_i(t)$ is obtained, we perform a Short-time Fourier-transform (STFT) [26]. Within each frame of the STFT, we perform quadratic interpolation to obtain the exact location of the peak [27, 26]. Figure 1 shows the results of our frequency tracking using the STFT for the second partial of a recorded high 'e' string. Note the pitch glide that occurs at the onset of the signal. As shown, there is a near 1 Hz difference between the initial frequency value and the steady-state value. Furthermore, the duration of the pitch glide is about one and a half seconds. In our analyses, we used a Hamming window of size 2^{15} samples, FFT length 2^{16} samples and 90 percent overlap. Figure 2 shows the normalized frequency trajectories of the first 15 partials of the same recording of the high 'e' string analyzed to produce Figure 1. We note that normalization corresponds to dividing the frequency trajectory by its steady-state/nominal frequency value. For the purposes of plotting, each

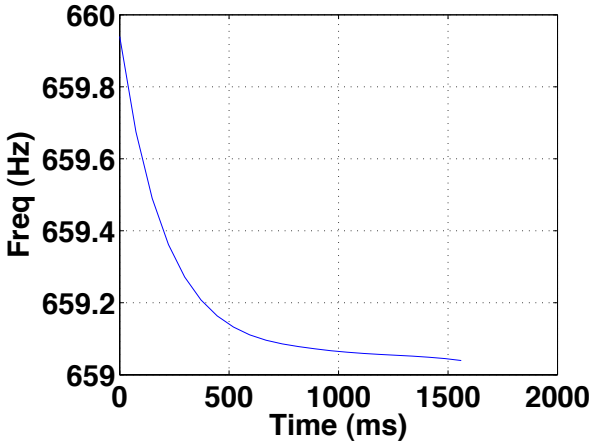

Figure 1: Pitch glide of the second partial of a recording of a high 'e' string.

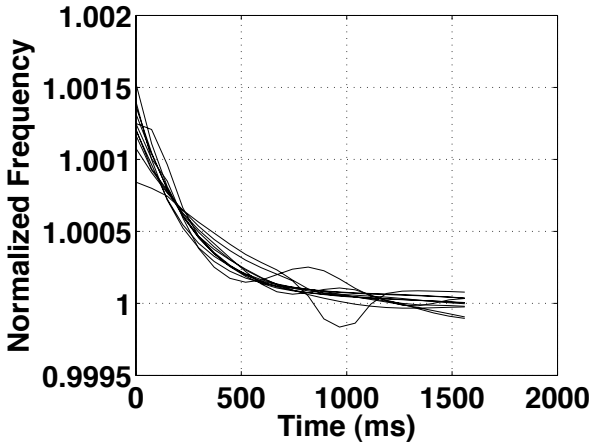

Figure 2: Pitch glide of the first 15 partials of a recording of a high 'e' string. Note the frequency trajectories have been normalized.

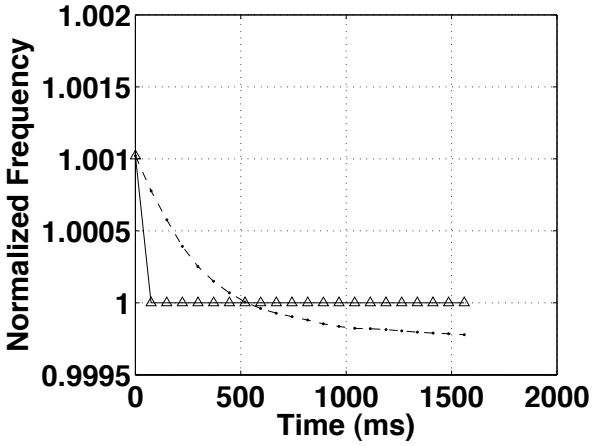

Figure 3: The dot-dashed curve shows the mean of the normalized frequency trajectories ($\eta(t)$) of the first 15 partials shown in Figure 2. The triangle-solid curve shows the fitted model with $\tau_0 = 0.005$ after one iteration.

trajectory is further shifted such that the mean steady-state frequency of each partial is one. Though the difference in frequency of the second partial over time is about a Hz over the span of a second and a half, we defer readers interested in the psycho-acoustic studies of the audibility of pitch glide to [28].

3. PITCH GLIDE MODEL

From the analyzed frequency trajectories in Section 2, we have found that the empirical measurements accurately match the following model:

$$\nu_i(t) = \nu_i(1 + \alpha e^{-t/\tau}) \tag{3}$$

where $\nu_i(t)$ corresponds to the frequency of partial i at time t, ν_i corresponds to the steady-state frequency of partial i and α and τ are parameters of our model.

From Eq. 3, when α is zero, our model exhibits no pitch glide. However, when α is non-zero, the exponential term yields the effect. Intuitively, when a string is plucked harder, α will be greater thus exhibiting greater pitch glide. Furthermore, setting $\alpha = e^{\beta/\tau}$, we can rewrite Eq. 3 as

$$\begin{aligned} \nu_i(t) &= \nu_i(1 + \alpha e^{-t/\tau}) \\ &= \nu_i(1 + e^{\beta/\tau} e^{-t/\tau}) \\ &= \nu_i(1 + e^{-(t-\beta)/\tau}) \end{aligned} \tag{4}$$

Therefore, as shown in Eq. 4, our α parameter corresponds exactly to our starting position on the decaying exponential with time-constant τ. More precisely, α determines the shift of the exponential curve to time zero.

3.1. Parameter Estimation

In this section, we present methods for obtaining τ and α of our pitch glide model described in Section 3. Since our optimization problem is nonlinear, we present an iterative method for solving for α and τ.

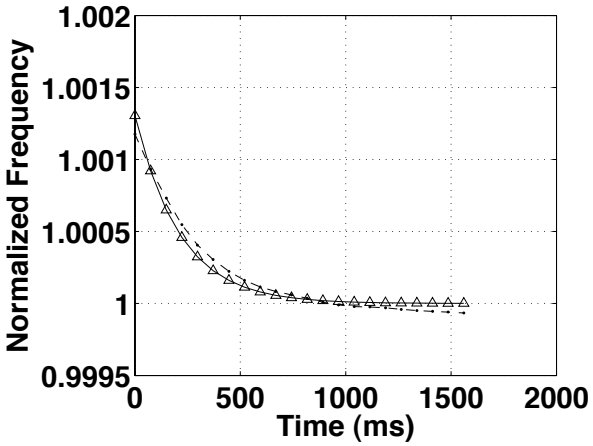

Figure 4: The dot-dashed curve shows the mean of the normalized frequency trajectories ($\eta(t)$) of the first 15 partials shown in Figure 2. The triangle-solid curve shows the fitted model with $\tau_2 = 0.209$ after two iterations.

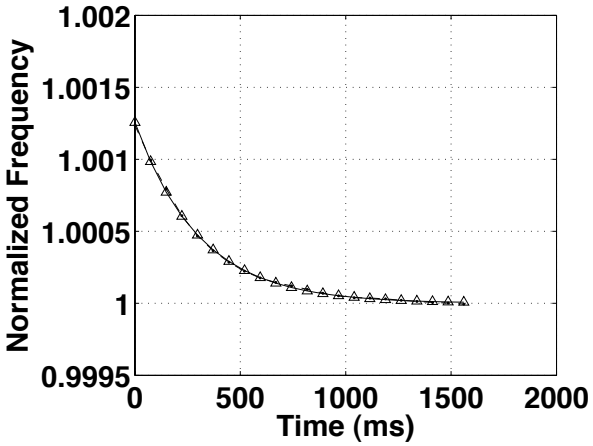

Figure 5: The dot-dashed curve shows the mean of the normalized frequency trajectories ($\eta(t)$) of the first 15 partials shown in Figure 2. The triangle-solid curve shows the fitted model with $\tau_{13} = 0.3049$ after convergence in 13 iterations. As shown, the model is a near perfect fit to the mean of the normalized frequency trajectories.

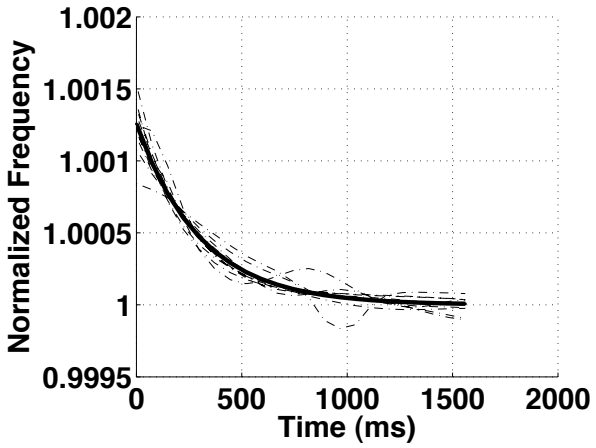

Figure 6: The multiple dashed-line curves show the normalized frequency trajectories of the first 15 partials also shown in Figure 2. The bold-solid curve shows the fitted model. As shown, the model fits the frequency trajectories well.

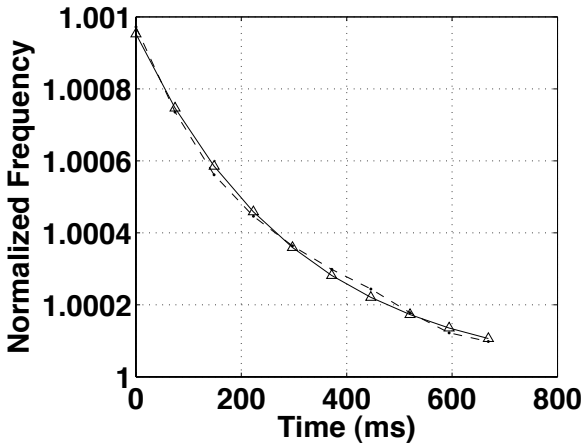

Figure 7: The dot-dashed curve shows the mean of the normalized frequency trajectories ($\eta(t)$) of the first 14 partials of an open high 'e' plucked at a lower amplitude. The triangle-solid curve shows our fitted model. Note that the same time constant, τ, computed for an open high 'e' plucked at a higher amplitude is used. However, α differs, corresponding to a shift in our pitch glide model curve. As shown, the model is a good approximation to the mean of the normalized frequency trajectories.

Given the frequency trajectories obtained in Section 2, we define the frequency trajectory for partial i as $\omega_i(t)$. We normalize each partial frequency trajectory by dividing by the minimum frequency value in that trajectory:

$$\omega_{i,norm}(t) = \omega_i(t) \Big/ \min_j \omega_i(j) \tag{5}$$

We now average the trajectory decays over time for all partials:

$$\eta(t) = \frac{1}{N} \sum_{i=1}^{N} \omega_{i,norm}(t) \tag{6}$$

We reformulate our model from Eq. 3 as follows such that normalized frequencies are used so that only a single optimization of the parameters of τ and α need be computed:

$$\begin{aligned} \nu_i(t) &= \nu_i(1 + \alpha e^{-t/\tau}) \\ \nu_i(t)/\nu_i &= 1 + \alpha e^{-t/\tau} \qquad (7) \\ \hat{\eta}(t) &= \phi_1 + \phi_2 e^{-t/\tau} \qquad (8) \end{aligned}$$

where $\alpha = \phi_2/\phi_1$. We reformulate our model to add an extra degree of freedom, so that given a value for τ, solving for the optimal values for ϕ_1 and ϕ_2 corresponds to a least squares formulation:

$$\min_{\phi_1,\phi_2} \sum_{t=0}^{T} (\eta(t) - \hat{\eta}(t))^2 \tag{9}$$

The solution to the optimization problem in Eq. 9, is shown in Eq. 12 and simply corresponds to the product of the pseudo-inverse of the matrix A and vector b, defined in Equations 10 and 11, respectively.

$$A = \begin{bmatrix} | & | \\ 1 & e^{-t/\tau} \\ | & | \end{bmatrix} \tag{10}$$

$$b = \begin{bmatrix} \eta(0) \\ \eta(1) \\ \vdots \\ \eta(T) \end{bmatrix} \tag{11}$$

$$\Phi = (A^T A)^{-1} A^T b \tag{12}$$

where $\Phi = \begin{bmatrix} \phi_1 \\ \phi_2 \end{bmatrix}$.

We now estimate τ by dividing b by ϕ_1, and fitting a straight-line to the initial points of $\log(b/\phi_1 - 1)$. We now set our new estimate for τ to be $\tau = -1/m$ where m corresponds to the slope of our fitted line.

We iterate, optimizing values for Φ and τ until successive values of τ differ by an optimization criterion. In practice, we stop our optimization when τ changes by less than 10^{-4}. Figure 3 shows our optimization after one iteration with $\tau_0 = 0.005$. Figure 4 shows our optimization after two iterations with $\tau_2 = 0.209$. Lastly, Figure 5 shows our fitted model after convergence in 13 iterations with $\tau = 0.3049$ over $\eta(t)$ and Figure 6 shows our fitted model over the normalized frequency trajectories of the first 15 partials.

3.2. A Softer Pluck

Using $\tau = 0.3049$ obtained in Section 3.1 for a recording of an open high 'e' string plucked at a high amplitude, we compare our model to a recording of an open high 'e' string plucked at a lower amplitude. Note that given a value for τ, we need simply compute α as described in Section 3.1, corresponding to the shift of our exponential curve. Figure 7 shows our fitted model with the same τ

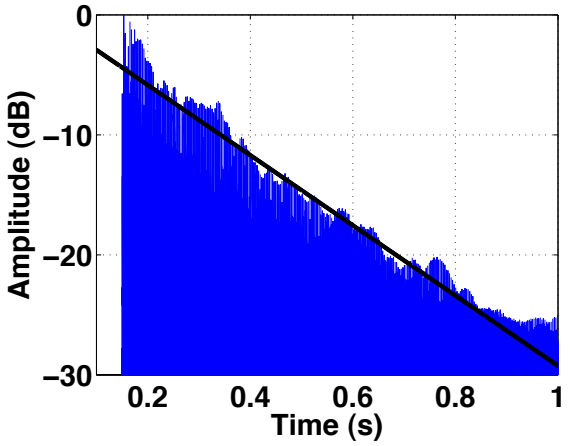

Figure 8: A line with slope $-2/\tau$, with τ computed in Section 3.1 is plotted over the square of the slope of the values of the signal in decibels. As shown, $-2/\tau$ corresponds well to the attenuation of the analyzed tone as expected.

computed from Section 3.1 but with a different fitted α parameter. Note that the pitch glide is significantly reduced, as is expected from a softer pluck.

3.3. Physicality of the Glide Model

As described in [5], the pitch glide time constant is related to the time constant of the attenuation of the tone. In this section, we relate the pitch glide model defined in Section 3 with the decay of waves on the string. We specify the speed of traveling waves on the string as follows:

$$c = \sqrt{\frac{T}{\epsilon}} \tag{13}$$

where T corresponds to the tension on the string and

$$\epsilon = m/L \tag{14}$$

where m corresponds to the mass of the string and L the length of the string.

We now define the fundamental frequency of the vibrating string as a function of the length of the string:

$$\begin{aligned} f(L) &= \frac{c}{2L} && (15)\\ &= \sqrt{\frac{T}{4mL}} && (16)\\ &\approx \sqrt{\frac{T}{4mL_0}} && (17) \end{aligned}$$

Note in Eq. 17, we assume that $L = L_0 + \delta L$ and that $\delta L << L_0$. We now relate the length of the string to the tension on the string:

$$L(T) = L_0 + \lambda T \tag{18}$$

Note that when the tension on the string is zero, the string resides at its nominal length L_0. Furthermore, this approximation corresponds to a small tension approximation so that the tension and length are linearly related [5]. Similarly, we can rewrite Eq. 18 so that tension is linear with respect to the change in string length.

$$T(L) = \frac{L - L_0}{\lambda} = \frac{\delta L}{\lambda} \tag{19}$$

We now substitute for tension, using Eq. 19, in Eq. 17:

$$\begin{aligned} f(L) &\approx [\frac{(L - L_0)/\lambda}{4mL_0}]^{1/2} && (20)\\ &= [\frac{\delta L/\lambda}{4mL_0}]^{1/2} && (21)\\ f(L_0 + \zeta) &\approx [\frac{\zeta/\lambda}{4mL_0}]^{1/2} && (22) \end{aligned}$$

As shown in Eq. 21, the fundamental frequency of the string increases according to the square-root of the increase in the length of the string. Note in Eq. 22, $f(L_0 + \zeta)$ corresponds to the nominal fundamental frequency of the string when the string is stretched such that its total length is $L_0 + \zeta$. We now define the length of the string with respect to the waveform on the string. When a string is displaced, its length increases. Therefore, we specify a time-varying length of the string with respect to the transversal displacement of the string with respect to time and space, $\psi(x, t)$, as follows:

$$\psi(x, t) \approx e^{-t/\tau} \cdot \mu(x) \tag{23}$$

where we assume that each point on the string exhibits a displacement $\mu(x)$ and the displacement decreases exponentially over time.

$$\begin{aligned} L(t) &= \int_0^{(L_0+\zeta)} \sqrt{(dx)^2 + (d\psi)^2} && (24)\\ &= \int_0^{(L_0+\zeta)} dx \cdot [1 + (\frac{d\psi}{dx})^2]^{1/2} && (25)\\ &\approx \int_0^{(L_0+\zeta)} dx(1 + \frac{1}{2}(\frac{d\psi}{dx})^2) && (26)\\ &= L_0 + \zeta + e^{-2t/\tau} \cdot \int_0^{(L_0+\zeta)} \frac{dx}{2}(\frac{d\mu(x)}{dx})^2|_{t=0} && (27)\\ &= L_0 + \zeta + e^{-2t/\tau} \cdot \gamma && (28) \end{aligned}$$

where we define

$$\gamma = \int_0^{(L_0+\zeta)} \frac{dx}{2}(\frac{d\mu(x)}{dx})^2|_{t=0}$$

Note that γ depends solely on the intial displacement of the string over x and is independent of time t.

We now substitute $L(t)$ from Eq. 28 into Eq. 17 to obtain a time-varying fundamental frequency.

$$\begin{aligned} f(t) &= f(L(t)) && (29)\\ &\approx [\frac{\zeta + e^{-2t/\tau} \cdot \gamma}{4mL_0\lambda}]^{1/2} && (30)\\ &\approx [\frac{\zeta}{4mL_0\lambda}]^{1/2}(1 + \frac{1}{2}e^{-2t/\tau} \cdot \gamma/\zeta) && (31) \end{aligned}$$

As Eq. 31 shows, the fundamental frequency as a function of time depends on the square of the slope of the displacement of

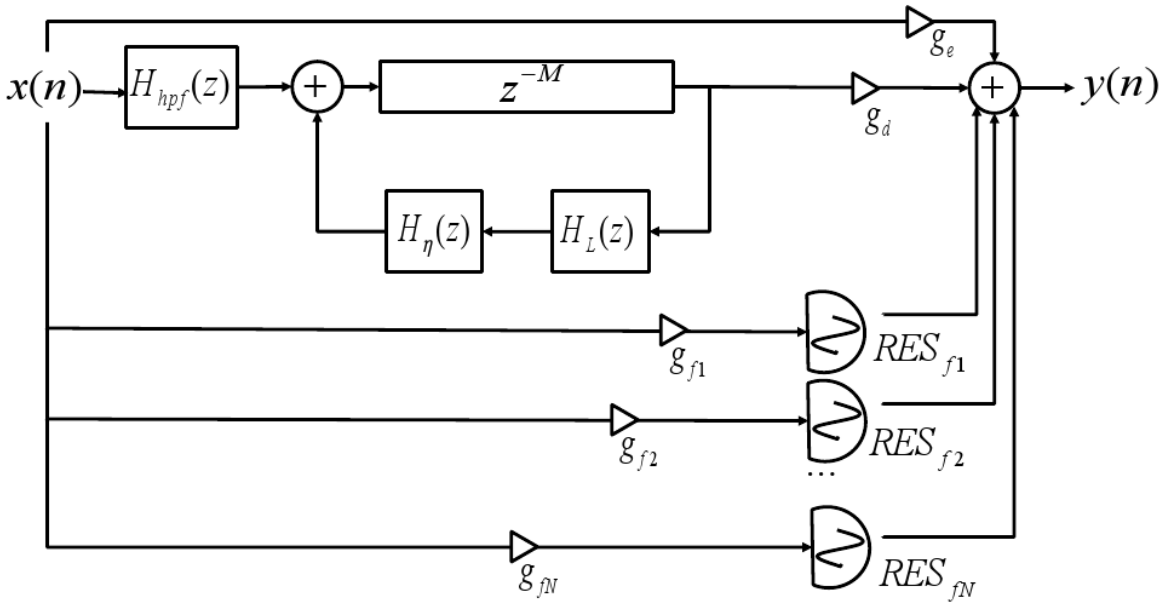

Figure 9: *Hybrid digital waveguide model with extended commuted synthesis highpass filter for excitation and parallel resonators for lower-partial realization.*

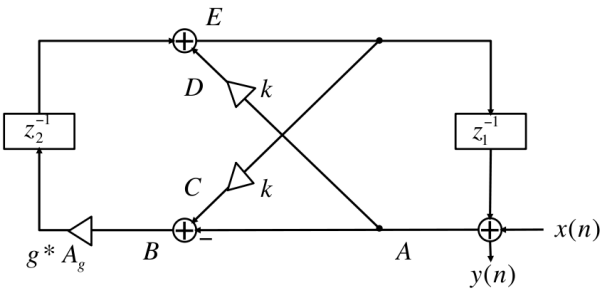

Figure 10: Block diagram of the recursive filter resonator used to implement all parameters of an exponentially-decaying sinusoid.

the string, which decays exponentially at time-constant $-2/\tau$. In Figure 8, a straight line with slope $-2/\tau$, with τ computed from Section 3.1 is plotted over the square of the space derivative of the same waveform analyzed in Section 3.1. As shown, the slope matches the decay well, thereby supporting the derivations outlined in this section and the physicality of the pitch glide model defined in Section 3.

4. THE SYNTHESIS MODEL

We propose a string synthesis model that is hybrid: a digital waveguide-modal synthesis model, similar to the digital-wavguide in parallel with a bank of resontars presented in [29]. Since the digital waveguide provides all partials up to half the sampling rate, we use a well-tuned digital waveguide to the correct fundamental frequency, and a bank of resonators to accurately model the lower, psychoacoustically significant partials.

In essence, complex characteristics such as beating and two-stage decay can be precisely modeled with two second-order resonators. However, we present a novel method negotiating the lower partials of the tone produced by the digital waveguide and the parallel bank of resonators. In [18], the bank of parallel second-order resonators are parameterized according to the partials generated by the digital waveguide. Rather than accommodate the partials produced by the digital waveguide, we remove them from our synthesis model. Instead of notch-filtering each partial or highpass filtering the output of the digital waveguide, we present a cost-free real-time implementation by high-pass filtering the excitation signal, therefore removing energy at the lower partials that would have otherwise been excited in the digital waveguide.

Analogous to concepts in commuted synthesis presented by [30, 31, 12], by high-pass filtering the excitation signal offline, removing the lower partials of the digital waveguide is free for real-time synthesis.

4.1. The Resonators

To implement the lower partials, we present second-order resonators that when impulsed, will reproduce the sinusoids of the original tone. However, the primary advantage of using second-order resonators is in re-exciting the string. The excitation signal is used to drive the resonators for string re-striking, and for creating a different tone per unique excitation with the same coupling parameters of the lower partials.

As Figure 9 shows, resonator $RES_{f,i}$ synthesizes partial i. Similar to [18], we propose a two-pole one-zero filter for each sinusoid. Therefore, partial i will consist of two independent resonators each implementing an exponentially-decaying sinusoid. If $\sigma_{i,j}$, $\omega_{i,j}$, $\theta_{i,j}$ and $r_{i,j}$ represent the exponential decay-rate, frequency, initial phase and initial magnitude of the jth sinusoid of partial i, the transfer function for the second-order resonator can

be written as follows:

$$H_{RES_{f,i,j}} = \frac{a_{i,j}}{1-p_{i,j}} + \frac{\bar{a}_{i,j}}{1-\bar{p_{i,j}}} \quad (32)$$

$$a_{i,j} = \frac{1}{2} \cdot r_{i,j} \cdot e^{j\theta_{i,j}} \quad (33)$$

$$p_{i,j} = g_{i,j} \cdot e^{j\omega_{i,j}} \quad (34)$$

$$g_{i,j} = e^{\sigma_{i,j}/fs} \quad (35)$$

4.2. Implementation Details

Implementation issues arise when changing the frequencies of oscillators. For example, using Direct-Form and its variant filter structures lead to artifacts such as amplitude modulation in the resulting signal.

To address this issue, we implement the resonators of our hybrid digital waveguide-modal synthesis model using recursive algorithms. As shown in Figure 10, the resonator structure used is described in [32] and is a variant of the structures described in [33].

Defining $\hat{x}_i(t)$ as our synthesis of the ith partial, Eq. 36 describes our model for a single partial.

$$\begin{aligned}\hat{x}_i(t) &= r_{i,1}e^{\sigma_{i,1}t}\cos(2\pi f_{i,1}(t)t + \theta_{i,1}) \ldots \\ &\quad + r_{i,2}e^{\sigma_{i,2}t}\cos(2\pi f_{i,2}(t)t + \theta_{i,2}) \end{aligned} \quad (36)$$

Thus, a single recursive resonator structure is used per exponentially-decaying sinusoid, resulting in two resonator structures per partial. We now relate the parameters of an exponentially-decaying sinusoid to the parameters of our resonator structure. Given an arbitrary initial amplitude, decay-rate, frequency and phase, r, σ, f and ϕ, respectively, we define the following parameters shown in Figure 10:

$$z_1^{-1}(0) = \cos(\phi) \quad (37)$$

$$z_2^{-1}(0) = -\sin(\phi) \cdot \sin(2\pi f_{nom}/fs) \quad (38)$$

We initialize our two delays as shown above in Equations 37 and 38 to account for the initial phase, ϕ. Note that fs corresponds to the sampling-rate. The decay-rate, σ, is implemented within the recursive filter structure as g, defined as follows:

$$g = e^{2\sigma/fs} \quad (39)$$

To account for the time-varying frequency, the structure implements a time-dependent gain that is defined as follows as A_ρ:

$$\rho(0) = \sin(2\pi f_{nom}/fs) \quad (40)$$

$$\rho(i) = \sin(2\pi f(i)/fs) \quad (41)$$

$$A_\rho = \rho(i)/\rho(i-1) \quad (42)$$

$$(43)$$

where f_{nom} corresponds to the steady-state frequency of the exponentially-decaying sinusoid and A_ρ depends on the current value of $\rho(i)$ and its previous value $\rho(i-1)$. The node signals defined as A,B,C,D and E are defined as follows:

$$k = \cos(2\pi f_{nom}/fs) \quad (44)$$

$$A = z_1^{-1}(i) + x(i) \quad (45)$$

$$D = k \cdot A \quad (46)$$

$$E = D + z_2^{-1}(i) \quad (47)$$

$$C = k \cdot E \quad (48)$$

$$B = C - A \quad (49)$$

and lastly our two delay samples are updated as follows:

$$z_1^{-1}(i+1) = E \quad (50)$$

$$z_2^{-1}(i+1) = g \cdot A_\rho \cdot B \quad (51)$$

$$y(i) = r \cdot E. \quad (52)$$

and our output at sample, $y(i)$, is defined above in Equation 52.

5. CONCLUSIONS

In this paper, we presented an empirical model that accurately describes the frequency trajectory of partials of a nonlinear string exhibiting pitch glide. Our model depends solely on the amplitude of the initial pluck of the tone. We also present methods for optimizing parameters of our model from recorded tones and integration of our pitch glide model into a hybrid digital-waveguide/modal-synthesis model with use of recursive algorithms.

6. REFERENCES

[1] G. F. Carrier, "On the nonlinear vibration problem of the elastic string," in *Q. Appl. Math*, 1945, vol. 3, pp. 157–165.

[2] G. V. Anand, "Large-amplitude damped free-vibration of a stretched string," *J. Acoust. Soc. Am.*, vol. 45, no. 5, pp. 1089–1096, 1999.

[3] J. A. Elliott, "Intrinsic nonlinear effects in vibrating strings," in *Am. J. Phys.*, 1980, vol. 48, pp. 478–480.

[4] C. Gough, "The nonlinear free vibration of a damped elastic string," in *J. Acoust. Soc. Am.*, 1984, vol. 75, pp. 1770–1776.

[5] K. A. Legge and N. H. Fletcher, "Nonlinear generation of missing modes on a vibrating string," in *J. Acoust. Soc. Am.*, 1984, vol. 76, pp. 5–12.

[6] A. Watzky, "Non-linear three-dimensional large-amplitude damped free vibration of a stiff elastic stretched string," *J. Sound and Vib.*, vol. 153, no. 1, pp. 125–142, 1992.

[7] C. Valette, "The mechanics of vibrating strings," in *Mechanics of Musical Instruments*, A. Hirschberg, J. Kergomard, G. Weinreich, and Springer-Verlag, Eds., pp. 115–183. New York: Springer Verlag, 1995.

[8] N. H. Fletcher and T. D. Rossing, *The Physics of Musical Instruments, 2nd Edition*, New York: Springer Verlag, 1998.

[9] T. Tolonen, V. Välimäki, and M. Karjalainen, "Modeling of tension modulation nonlinearity in plucked strings," *IEEE Transactions on Speech and Audio Processing*, vol. 8, no. 3, pp. 300–311, May 2000.

[10] C. Erkut and V. Välimäki, "Model-based sound synthesis of tanbur, a Turkish long-necked lute," in *Proceedings of the IEEE International Conference on Acoustics, Speech, and Signal Processing*, Istanbul, Turkey, June 5-9 2000, vol. 2, pp. 769–772.

[11] N. Lee, A. Chaigne, J. O. Smith III, and K. Arcas, "Measuring and understanding the gypsy guitar," in *International Symposium on Musical Acoustics*, Barcelona, Spain, September 9-12, 2007.

[12] J. O. Smith III, *Physical Audio Signal Processing for Virtual Musical Instruments and Audio Effects*, http://ccrma.stanford.edu/˜jos/pasp/, Dec. 2008, online book.

[13] J. O. Smith III, "Physical modeling using digital waveguides," in *Computer Music Journal*, 1992, vol. 16, pp. 74–91.

[14] V. Välimäki, J. Pakarinen, C. Erkut, and M. Karjalainen, "Discrete-time modelling of musical instruments," *Reports on Progress in Physics*, vol. 69, no. 1, pp. 1–78, Jan. 2006.

[15] T. I. Laakso, V. Välimäki, M. Karjalainen, and U. K. Laine, "Splitting the unit delay–tools for fractional delay filter design," in *IEEE Signal Processing Magazine*, January 1996, vol. 13, pp. 30–60.

[16] S. Tassart, R. Msallam, P. Depalle, and S. Dequidt, "A fractional delay application: Time-varying propagation speed in waveguides," in *Proceedings of the International Computer Music Conference*, Thessaloniki, Greece, Sept 1997, pp. 256–259.

[17] V. Välimäki, T. Tolonen, and M. Karjalainen, "Signal-dependent non-linearities for physical models using time-varying fractional delay filters," in *Proceedings of the International Computer Music Conference*, Ann Arbor, MI, Oct 1998, pp. 264–267.

[18] B. Bank, *Physics-Based Sound Synthesis of the Piano*, Number Report 54. Helsinki University of Technology, Laboratory of Acoustics and Audio Signal Processing, May 2000.

[19] S. Bilbao, "Energy-conserving finite difference schemes for tension-modulated strings," in *Proceedings of the IEEE International Conference on Acoustics, Speech, and Signal Processing*, Montreal, Canada, May 2004, vol. 4.

[20] S. Bilbao, "Conservative numerical methods for nonlinear strings," *Journal of the Acoustical Society of America*, vol. 118, no. 5, pp. 3316–3327, 2005.

[21] J. Pakarinen, M. Karjalainen, V. Välimäki, and S. Bilbao, "Energy behavior in time-varying fractional delay filters for physical modeling synthesis of musical instruments," in *Proceedings of the IEEE International Conference on Acoustics, Speech, and Signal Processing*, Philadelphia, PA, March 2005, vol. 3.

[22] S. Bilbao, "Time-varying generalizations of all-pass filters," *IEEE Signal Processing Letters*, vol. 12, no. 5, May 2005.

[23] J. Pakarinen, M. Karjalainen, and V. Välimäki, "Modeling and real-time synthesis of the kantele using distributed tension modulation," in *Proceedings of the Stockholm Music Acoustics Conference*, Stockhom, Sweden, August 6-9 2003, pp. 409–412.

[24] L. Trautmann and R. Rabenstein, "Sound synthesis with tension modulated nonlinearities based on functional transformations," in *Acoustics and Music: The Theory and Applications*, N.E. Mastorakis, Ed., Jamaica, Dec. 2000, pp. 444–449.

[25] H. M. Lehtonen, V. Välimäki, and T. I. Laakso, "Canceling and selecting partials from musical tones using fractional delay filters," *Computer Music Journal*, vol. 32, no. 2, pp. 43–56, 2008.

[26] Julius Orion Smith III, *Spectral Audio Signal Processing*, http://ccrma.stanford.edu/˜jos/sasp/, Mar. 2009, online book.

[27] M. Abe and J. O. Smith III, "Design criteria for simple sinusoidal parameter estimation based on quadratic interpolation of FFT magnitude peaks," *Audio Engineering Society Convention, San Francisco*, 2004, Preprint 6256.

[28] H. Järveläinen and M. Karjalainen, "Perceptibility of inharmonicity in the acoustic guitar," in *ACTA Acustica United with Acustica*, 2006, vol. 92, pp. 842–847.

[29] B. Bank, V. Välimäki, L. Sujbert, and M. Karjalainen, "Efficient physics based sound synthesis of the piano using dsp methods," in *Proceedings of the European Signal Processing Conference (EUSIPCO00)*, 2000, vol. 4, pp. 2225–2228.

[30] J. O. Smith III, "Efficient synthesis of stringed musical instruments," in *Proceedings of the 1993 International Computer Music Conference*, Tokyo, Japan, 1993, pp. 64–71.

[31] M. Karjalainen, V. Välimäki, and Z. J'anosy, "Towards high-quality sound synthesis of the guitar and string instruments," in *Proceedings of the 1993 International Computer Music Conference*, Tokyo, Japan, Sept. 10-15 1983, pp. 56–63.

[32] J. Nam, "A study of sinusoid generation using recursive algorithms," in *Journal of Korean Electro-Acoustic Music Society*, December 2005.

[33] J. O. Smith III and P. R. Cook, "The second-order digital waveguide oscillator," in *Proceedings of the International Computer Music Conference*, San Jose, October 1992, pp. 150–153.

[34] M. Karjalainen, V. Välimäki, and T. Tolonen, "Plucked-string models: From the Karplus-Strong algorithm to digital waveguides and beyond," *Computer Music Journal*, vol. 22, no. 3, 1998.

[35] V. Välimäki., J. Huopaniemi, M. Karjalainen, and Z. Jánosy, "Physical modeling of plucked string instruments with application to real-time sound synthesis," *Journal of the Audio Engineering Society*, vol. 44, no. 5, pp. 331–353, May 1996.

[36] V. Välimäki. and T. Tolonen, "Development and calibration of a guitar synthesizer," *Journal of the Audio Engineering Society*, vol. 46, no. 9, pp. 766–778, September 1998.

[37] D. A. Jaffe and J. O. Smith, "Extensions of the Karplus-Strong plucked string algorithm," *Computer Music Journal*, vol. 7, no. 2, pp. 56–69, 1983.

[38] J. C. Risset, "Computer music experiments, 1964–„" *Computer Music Journal*, vol. 9, no. 1, pp. 11–18, 1985.

[39] N. Lee, Z. Duan, and J. O. Smith III, "Excitation extraction for guitar tones," in *Proceedings of the 2007 International Computer Music Conference*, Copenhagen, Denmark, August 27-31 2007.